Journal of Hazardous Materials 186 (2011) 1226–1233

Contents lists available at ScienceDirect

Journal of Hazardous Materials

journal homepage: www.elsevier.com/locate/jhazmat

Laser induced photocatalytic degradation of hazardous dye (Safranin-O) using self synthesized nanocrystalline WO_3

K. Hayat [a], M.A. Gondal [b,*], M.M. Khaled [a], Z.H. Yamani [b], S. Ahmed [c]

[a] Chemistry Department, King Fahd University of Petroleum & Minerals, Dhahran 31261, Saudi Arabia
[b] Laser Research Group, Physics Department and Center of Excellence in Nano Technology (CENT), King Fahd University of Petroleum & Minerals, Box 372, Dhahran 31261, Saudi Arabia
[c] Center for Petrochemical and Refining, Research Institute, King Fahd University of Petroleum & Minerals, Dhahran 31261, Saudi Arabia

ARTICLE INFO

Article history:
Received 6 May 2010
Received in revised form 8 October 2010
Accepted 30 November 2010
Available online 8 December 2010

Keywords:
Safranin-O
Waste water treatment
Laser applications
Photocatalysis
Nanocrystalline WO_3

ABSTRACT

The photocatalytic degradation of Safranin-O (known as Basic Red 2) in water using locally synthesized nanocrystalline WO_3 as a photocatalyst was investigated under UV laser irradiation. The photo-oxidation removal of the dye was monitored by UV–vis spectrophotometer. The blank experiments for either laser irradiated only Safranin-O solution or the suspension containing WO_3 and Safranin-O in the dark showed that both laser illumination and the photocatalyst were essential for the removal of Safranin-O. The effect of experimental parameters including laser energy, catalyst loading, solution pH and the initial dye concentration on photocatalytic degradation of Basic Red 2 were also investigated. Results indicate that the rate of reaction is strongly influenced by the adsorption of an azo dye into the surface of the photocatalyst materials and suggests an optimum catalyst loading and dye concentration for the degradation reaction. It was investigated that the adsorption of the dye decreases at higher alkaline pH because both catalyst and substrate are negatively charged, developing repulsive forces between them. Kinetic data obtained reveals that the rate of the reaction obeys the first-order kinetics.

1. Introduction

Dyes are an important class of chemicals which are widely used in many industrial processes in the leather, textile and printing industries. The discharge of these dyes in the effluents by these industries may cause a major environmental problem by contaminating the water reservoir [1,2]. Most of these dyes are major environmental concern because of their known carcinogenic properties [3]. As a result of this, various chemical and physical treatment processes have been developed including precipitation, adsorption, air stripping, flocculation, reverse osmosis and ultra filtration. These processes are not cost effective since they only transfer the non-biodegradable matter into sludge, giving rise to new problems which need further treatment [4,5]. Advanced oxidation processes are best alternatives for removal of dyes and many other persistent organic and effluents from wastewater. These processes generally, involve UV/H_2O_2, UV/O_3 or UV/Fenton's reagent for the oxidative degradation of contaminants. Heterogeneous photocatalysis has emerged as an effective technique for the removal and degradation of pollutants of organic, biological and inorganic origins leading to the total mineralization of these pollutants [6–9].

Among advanced oxidation processes, semiconductor photocatalysis has emerged an important destructive technology leading to the total mineralization of most of the organic pollutants [10]. The ability of the semiconductor to enhance the photodegradation of the dye is attributed to its electronic structure which is characterized by filled valence band and an empty conduction band. When the semiconductors are illuminated with energy greater than their band gap energy (E_g) excited high-energy states of electron (e^- CB) and hole ($h\nu B^+$) pairs are produced.

$$SC + h\gamma \rightarrow Sc(e^-CB + h\nu B^+) \quad (1)$$

where SC = semiconductor (metal oxide)

$$e^-CB + O_2 \rightarrow O_2^{\bullet -} \quad (2)$$

$$h\nu B^+ + H_2O \rightarrow H^+ + OH^\bullet \quad (3)$$

$$OH^\bullet + \text{dye} \rightarrow H_2O + \text{Dyeintermediate} \quad (4)$$

$$\text{Dyeintermediate} + OH^\bullet \rightarrow CO_2 + H_2O \quad (5)$$

The reason for the large interest in this process is the use of atmospheric air as an oxidant and sun light under ambient conditions. Moreover, this process utilizes cheaply available nontoxic semiconductors (TiO_2, ZnO, WO_3) and leads to total mineralization of organic compounds to environmental friendly compounds like CO_2, and water. Many studies have been reported on the pho-

* Corresponding author. Tel.: +966 38602351; fax: +966 38602293.
E-mail address: magondal@kfupm.edu.sa (M.A. Gondal).

0304-3894/$ – see front matter © 2010 Elsevier B.V. All rights reserved.
doi:10.1016/j.jhazmat.2010.11.133

tocatalytic degradation of refractory organics. Degussa P-25 TiO_2 has been used for many systems either in suspended or in supported forms [11]. In few studies, other semiconductors, such as ZnO [12,13] and CdS [14] have also been applied.

The aim of the present work is to investigate the potential of nanocrystalline WO_3 as a photocatalyst under unique source (laser) of UV radiation for the oxidation of textile dyes in aqueous solutions. Safranin-O (C.I name is Basic Red 2) is a representative example of an organic dye, which belongs to the quinone–imine class, and is widely used for counterstaining purposes, for example, as a metachromatic method for cartilages which is stained yellow. Since the dye is known to be carcinogenic in nature, any presence of this dye in wastewater would have detrimental effects on marine environment. Effects of different operational parameters such as catalyst-loading, initial dye concentration, pH, and UV radiation intensity on the rate of photodegradation of the dye were studied. These are the major variables governing the efficiency of the process. The initial rates of reaction were calculated for various initial dye concentrations. The observesd data obey the first order kinetic model. The Chemical structure of the dye was shown below.

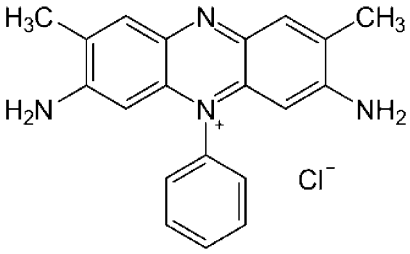

Chemical structure of Safranin O

2. Materials and methods

2.1. Materials

The commercial azo dye Safranin-O, obtained from Colour Chem, Pondicherry, was used without further purification. The absorption spectrum of Safranin-O is given in Fig. 1.The Nanocrystalline WO_3 was synthesized by precipitation method. It has a particle size 31 nm as estimated by XRD. $HClO_4$, NaOH were used to adjust the pH of the solution whenever was necessary. Deionized water was used throughout this work.

2.2. Synthesis of nano WO_3

The WO_3 nanostructures were synthesized by precipitation technique from aqueous solution of ammonium tungstate pentahydrate ($(NH_4)_{10}{\cdot}W_{12}O_{41}{\cdot}5H_2O$) and nitric acid ($HNO_3$, Merck). WO_3 nanoparticles were synthesized by the precipitation method as reported by Supothina et al. [15]. A pre-determined amount of the tungstate salt was dissolved in deionized water and the resulting solution was heated up to 85 °C slowly. Appropriate amount of a warm, concentrated nitric acid was added dropwise to this solution with continuous vigorous stirring. The mixed solution was kept at 85 °C for 25 min under continuous stirring conditions. The precipitate was allowed to settle for 24 h at room temperature. The precipitate was washed by addition of a large amount of deionized water followed by stirring for about 15 min and allowing the precipitates to settle down for 24 h before decanting the liquid. This same washing procedure was carried out for three times. Finally, the precipitates were separated by ultra-filtration procedure by using a polymer membrane (pore size = 0.2 μm). Then, the precipitate was dried at 80 °C for 24 h. After drying, it was calcined at 500 °C for 7 h at the rate of 1 °C/min. The synthesized nanostructure WO_3 in powder form was then characterized.

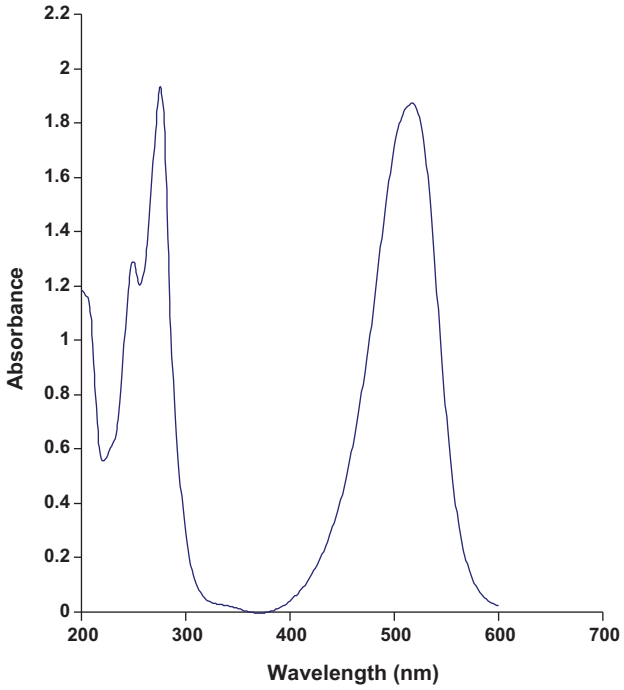

Fig. 1. Typical UV absorption spectrum for Basic Red 2.

2.3. Characterization

The morphologies of the synthesized WO_3 were characterized using transmission electron microscopy (TEM, JEM 200CX, 120 kV) and scanning electron microscopy (SEM, Hitachi S-4700 II, 25 kV). Size and morphologies of the synthesized WO_3 nanopowder is presented in the TEM images as depicted in Fig. 2. TEM images of synthesized WO_3 showed that most of the particles are plate like in shape ranging from 50 to 100 nm, while some of the particles are cylindrical as shown in SEM image (Fig. 3). The mean particle size of nano WO_3 was 50 nm as investigated by SEM. The energy dispersive spectrometry (EDS) analysis was employed to determine the composition of the tungsten oxide. As depicted in Fig. 4, only oxygen and tungsten elements existed in the nanoparticles of WO_3 with molar ratio of about 3 (O/W).

The X-ray diffraction (XRD) measurements were performed using a Bruker X-ray diffractometer in the range of 10–70 (2θ), using a monochromatized Cu Kα radiation (λ = 0.154 nm). A representative XRD pattern for our synthesized tungsten oxide is presented in Fig. 5. All the main peaks can be indexed to hexagonal WO_3 (JCPDS card 35-1001) which are consistent with general features of nanomaterials. Diffraction peaks of (0 0 1) are stronger compared with the rest, indicating that the [0 0 1] is the major growth direction. The crystallite size was calculated from peak broadening (in nm) using the Scherrer approximation [16], which is defined as

$$t = \left[\frac{0.9\lambda}{B\cos\theta}\right]$$

where λ is the wavelength of the X-ray (15.418 nm), B is the full width at half maximum (FWHM, radian) and θ is the Bragg angle (°). The FWHM value was obtained by performing profile fitting using an XRD pattern processing software. Scherrer's equation lead to average particle size of 31 nm for the WO_3 calcined at 500 °C which is in conformity with the results obtained from TEM

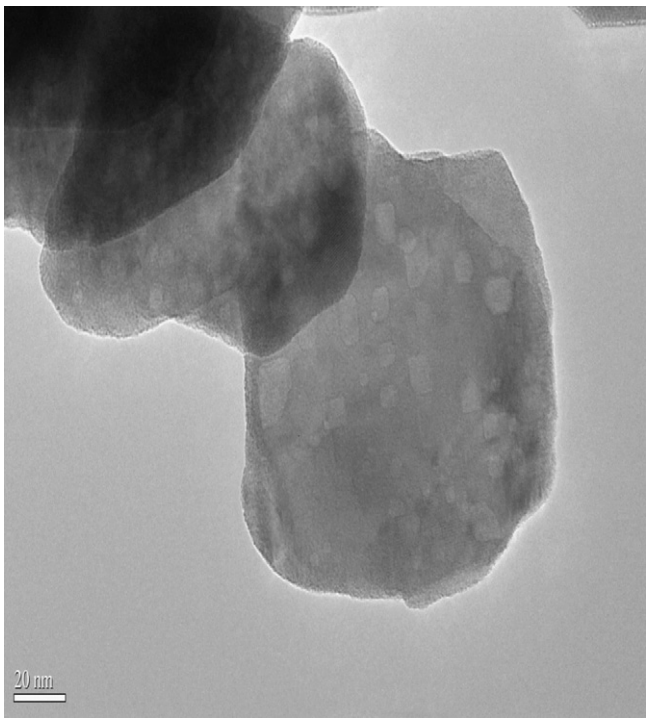

Fig. 2. TEM image of nanocrystalline WO_3 calcined at 500 °C.

and SEM. EDS analyses fairly agreed with the stoichiometry of the synthesized compound.

2.4. Photocatalytic activity

The experimental setup designed locally for the study of removal of dye from water using laser induced photocatalysis process is described in detail in our earlier publications [17,18]. A

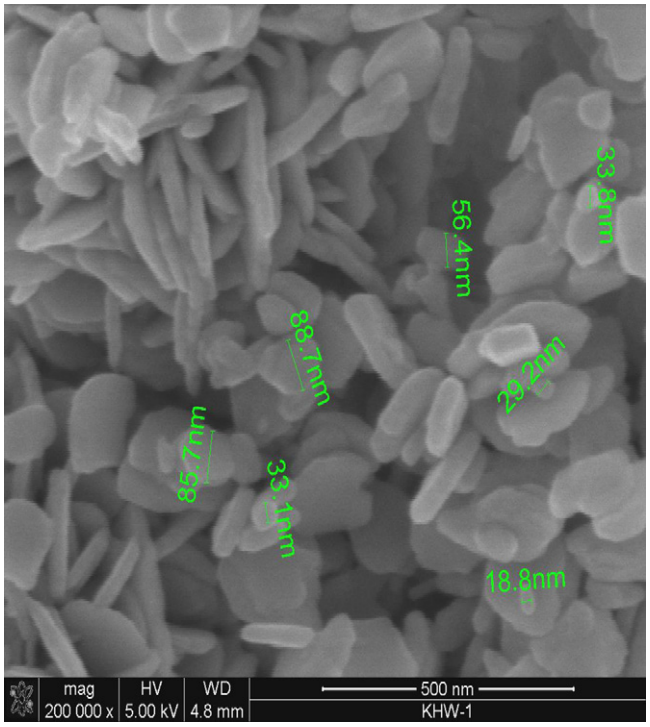

Fig. 3. SEM image of nanocrystalline WO_3 calcined at 500 °C.

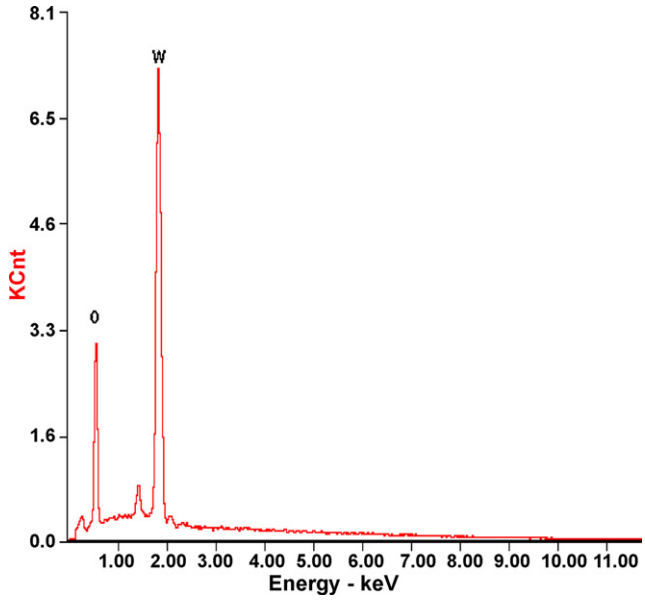

Fig. 4. EDX of nanocrystalline WO_3.

stock solution containing 200 mg L^{-1} of the dye was prepared to investigate the photocatalytic degradation of Safranin-O. 100 mg of nanocrystalline WO_3 was added to 100 mL of the dye solution and allowed to equilibrate for 15 min without laser irradiation. Then the sample was irradiated using the third harmonic at $\lambda = 355$ nm generated from Nd:YAG laser. The photochemical reaction was carried out in batches. During irradiation, the glass reactor was mounted on a magnetic stirrer to keep the suspension homogenous and after regular time intervals, 5 mL of the sample was withdrawn by the syringe and filtered using 0.2 μm Millipore membranes. The photocatalytic removal of the dye from water was monitored by recording the changes in the absorption spectra of Safranin-O at different laser irradiation times with a UV–vis spectrophotometer in the wavelength range from 200 to 700 nm. The data

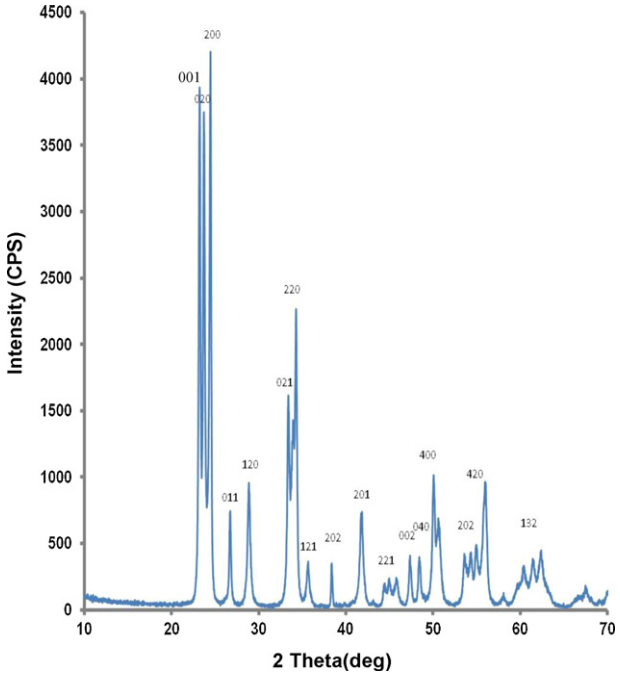

Fig. 5. X-ray diffractrogram for nanocrystalline WO_3.

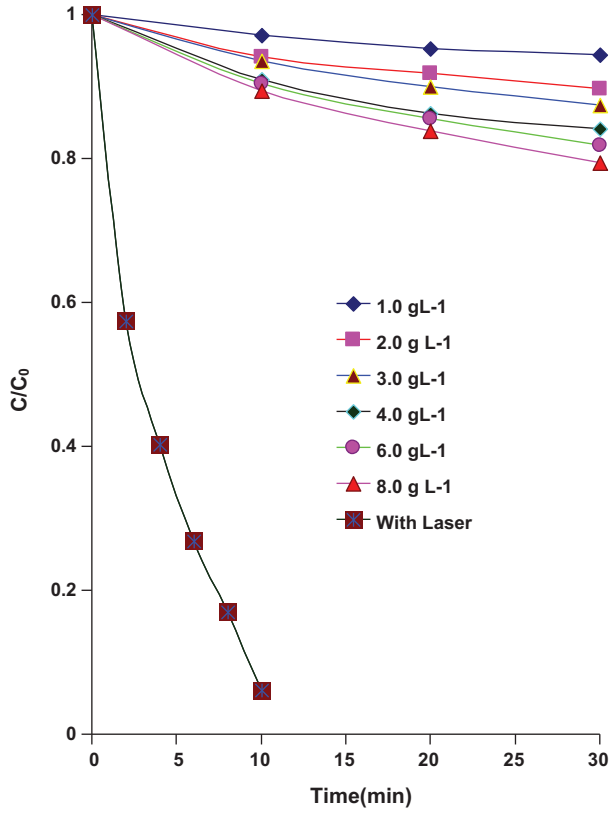

Fig. 6. A plot showing the comparison of dye removal by adsorption with different amount of catalyst and photocatalytic degradation using laser.

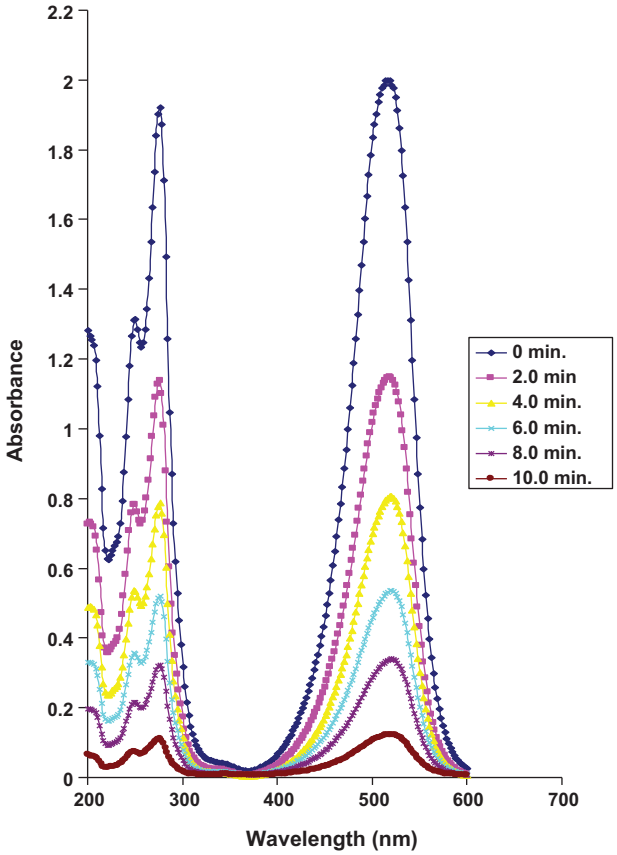

Fig. 7. Typical UV–visible spectra showing the change in absorption intensity as a function of laser exposure time for an aqueous solution of Basic Red 2 in presence of WO_3. Experimental conditions: dye concentration = 0.57 mM, V = 100 mL, WO_3 = 1.0 g L^{-1}, pH 8.2 laser energy = 140 mJ, laser exposure time = 10 min.

obtained was used to estimate the rate of the photo degradation of Safranin-O.

3. Results and discussions

3.1. Effect of laser UV irradiation and photocatalyst

Since some dyes are photo-degraded by direct UV irradiation. Therefore, prior to study the photo-catalytical removal, it was observed to what extent the dye (BR2) is degraded under UV laser irradiation without the presence of catalyst. For this purpose, blank experiments were carried out for the dye solution without catalyst. No significant degradation (less than 5.0%) was observed without the catalyst. The adsorption of the dye under different amount of catalyst was investigated. The results obtained and comparison of only adsorption and photocatalytic degradation is depicted in Fig. 6. The adsorption of Safranin-O increases as the amount of the catalyst increases from 1.0 g L^{-1} to 8.0 g L^{-1} ranging from ~5% to 19% even after 30 min but 94.0% degradation was achieved within 10 min using 1.0 g L^{-1} WO_3 .under laser induced phtotocatalytic process which is considered very high as compared with adsorption alone with out laser irardition.

Fig. 7 shows the change in absorption intensity as a function of laser irradiation time of an aqueous solution of Basic Red 2 (BR2) in the presence of nano-structured WO_3. Fig. 8 shows a plot of $\ln C_0/C$ versus laser irradiation time for an aqueous solution of dye (BR2) in presence of nanocystalline WO_3 and fitted data for the first order degradation kinetics of BR2.

The concentration of BR2 was 0.57 mM. It is evident from the results depicted in Fig. 9 that 94.0% degradation was achieved within very short laser irradiation time (10 min) using 355 nm laser, a coherent UV irradiation source. These results indicate that

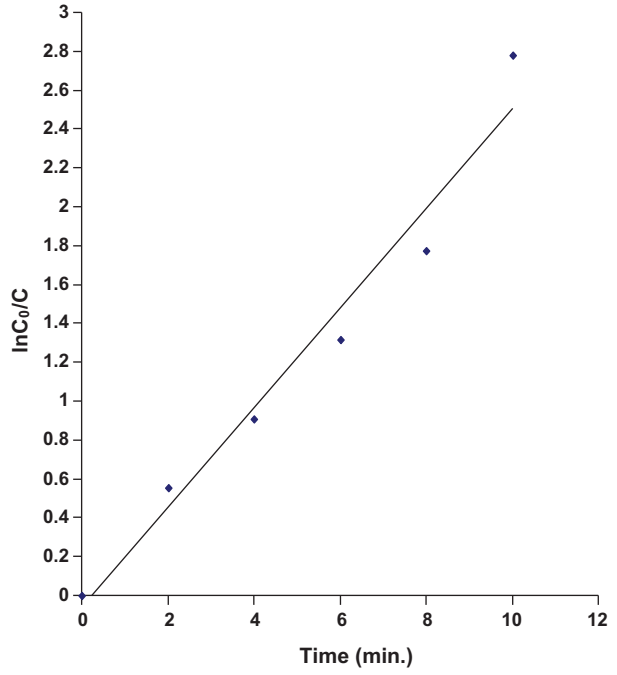

Fig. 8. A plot of $\ln C_0/C$ versus laser irradiation time for an aqueous solution of BR2 in presence of nanocystalline WO_3 and curve fit data for the first order degradation kinetics of BR2.

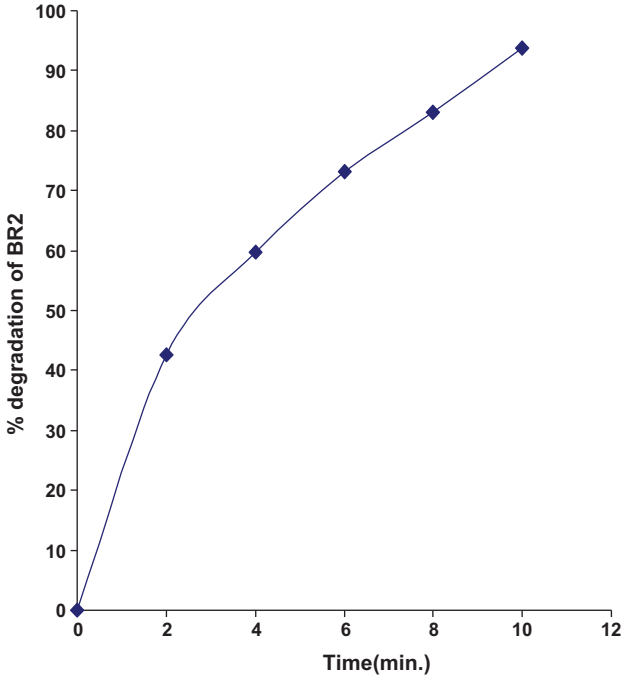

Fig. 9. The diagram showing the % degradation of BR2 with the increase in irradiation time.

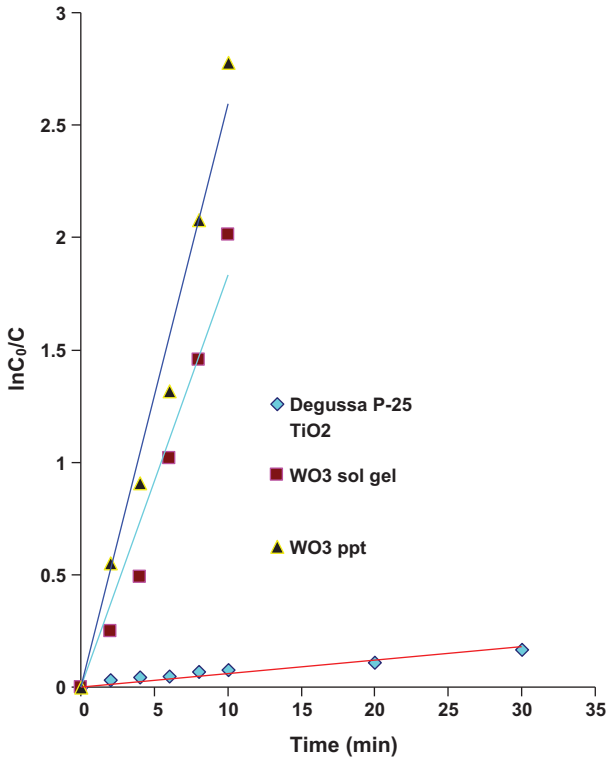

Fig. 10. A graph showing $\ln C_0/C$ versus laser irradiation time for an aqueous solution of BR2 in presence of Degussa P-25 TiO_2, nanocystalline WO_3 prepared by ppt method and nanocystalline WO_3 synthesized by sol–gel method.

both UV laser light and photocatalyst are essential for the effective removal of the dye.

3.2. Kinetics of photocatalytic degradation of Basic Red 2

The results of photocatalytic degradation of Basic Red 2 under laser UV irradiation over WO_3 are depicted in Fig. 7. The degradation rate for the decomposition of the dye under investigation was calculated [19,20] using the formula given below,

$$\frac{-d[C]}{dt} = kC^n \quad (6)$$

where C = concentration of Safranin-O remaining after time t, k = rate constant and n = order of reaction. A typical plot of $\ln C_0/C$ versus laser irradiation time is depicted in Fig. 8 for dye degradation. The least square fit, $r^2 = 0.9649$ and rate constant = 0.2566 min^{-1} as estimated from Fig. 8 are also indicted. This photodegradation rate could be considered very high as compared with the reported values using conventional setups using broad band spectral sources like lamps. A plot of percentage dye degradation (Safranin-O) removal is depicted in Fig. 9. Almost 94.0% removal of Safranin-O was achieved during only 10 min laser irradiation using nanocrystalline WO_3 semiconductor catalyst which is very high in this short span of time.

The results regarding the comparison of the rates for Degussa P-25 TiO_2, WO_3 ppt and WO_3 sol–gel are depicted in Fig. 10.The rate constant for photocatalytic degradation of Safranin-O using WO_3 synthesized by ppt method,WO_3 synthesized by sol–gel and Degussa P-25 TiO_2 obtained are 0.2595 min^{-1}, 0.1835 min^{-1} and 0.006 min^{-1} respectively. The sample prepared by precipitation method showed better degradation rate as compared to WO_3 synthesized by sol–gel method. The experiments were done using the laser irradiation (355 nm). Degussa P-25 TiO_2 exhibit lower photodegradation of Safranin-O at this wavelength (355) nm because it may not absorb the light radiations generated from third harmonic at λ = 355 nm (Nd:YAG laser). This could be due to the unsuitability of band gap of TiO_2 at 355 nm.

The results indicate that the percentage degradation of Basic Red 2 increases with the increase in laser irradiation time. This increase in degradation of Safranin-O with time could be due to the fact that with increase in the laser irradiation time, the number of absorbed laser photons increases, producing more amount of OH radicals, thereby facilitating more degradation of the dye.

3.3. Effect of laser energy

The effect of incident laser energy on the photocatalytic degradation of the dye was investigated and the results obtained are presented in Table 1. The results indicate that the degradation of the dye was significantly influenced by the laser energy and photodegradation of BR2 was increased almost linearly with the increase in laser energy up to a certain energy level as shown in Fig. 11. When 140 mJ of laser energy was applied, maximum 94% degradation was recorded within 10 min of irradiation and a fur-

Table 1
Laser induced photocatalytic degradation of Basic Red 2 in aqueous suspensions of nanocrystalline WO_3 under different operational parameters.

S.No.	Parameters	Rate constant (min^{-1})	Photodegradation rates (mM min^{-1})
1	Initial pH		
	5.0	0.169	0.096
	8.0	0.246	0.140
	10.0	0.314	0.179
	11.6	0.012	0.007
2.	Energy (mJ)		
	40	0.0128	0.0073
	70	0.0515	0.0294
	100	0.173	0.0986
	140	0.256	0.1459
	170	0.405	0.2308
	200	0.701	0.3996

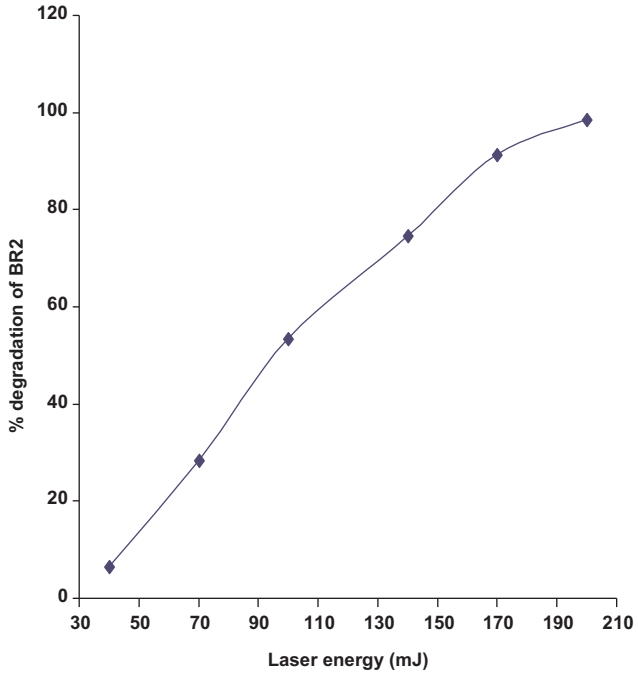

Fig. 11. Percentage removal of Basic Red 2 as a function of laser energy for nanocrystalline WO_3.

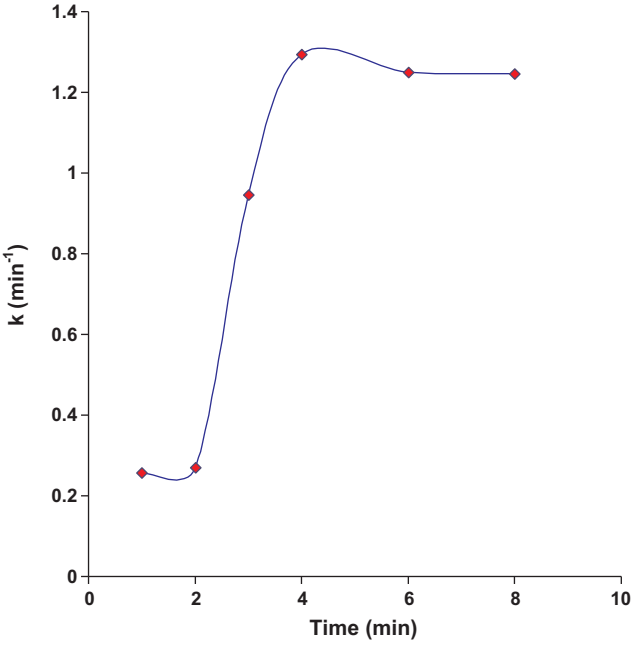

Fig. 12. Effect of catalyst concentration on photocatalytic degradation of BR2.

ther increase in the laser energy was not found to be beneficial for the degradation of the dye. This phenomenon may be explained in terms of the fact that when laser energy is increased, incident photon flux increases in the solution exciting more and more catalyst particles which, in turn, increases the degradation of the dye. The influence of laser energy on the rate of dye decolorization was examined at constant initial dye concentration ($C_0 = 5.7 \times 10^{-4}$ M, pH 8.2) and catalyst loading (WO_3 = 1000 mg L^{-1}). The dependency of photocatalytic removal of the dye on the light intensity observed in this study followed similar trend as explained in earlier studies [21,22] in which, it was concluded that there is a linear relationship between the rate and the light intensity up to a certain level.

3.4. Effect of catalyst concentration

The effect of photocatalyst concentration was studied by varying catalyst concentration from 1.0 to 8.0 g L^{-1} for the dye solutions of 0.57 mM at natural pH. The degradation efficiency for various catalysts loading for Basic Red 2 has been depicted in Fig. 12. The results reveal that the rate constant increases greatly by increasing the catalyst loading from 1.0 to 4.0 g L^{-1} for the dye, the rate of photodegradation remains almost constant for the higher catalyst loading. This can be explained on the basis that optimum catalyst loading is found to be dependent on initial solute concentration because with the increase of catalyst dosage, total active surface area increases, hence availability of more active sites on catalyst surface. The photocatalytic destruction of other organic pollutants has also exhibited the same dependency on catalyst dose [23]. At the same time, due to an increase in turbidity of the suspension with high dose of photocatalyst, there will be a decrease in penetration of UV light and hence photo activated volume of suspension decreases [24]. This limit, therefore, depends on the nature and concentration of organic contaminants and the working conditions of photo reactor. When the catalyst concentration is very high, the efficiency of the catalyst is hindered by the turbidity of suspension which decreases the penetration of light in the reactor. Thus it could be concluded that the higher dose of catalyst may not be useful both in view of aggregation as well as reduced irradiation field due to light scattering. Therefore the catalyst dose 1.0 g L^{-1} was fixed for further studies.

In order to assess the recyclability of WO_3 prepared by ppt method experiments were carried out under the identical conditions as applied for the evaluation of photocatalytic activity of different fresh catalysts for the degradation of the dye under investigation. After the completion of the reaction (cycle I), the WO_3 catalyst was collected and utilized for the second and third cycle under the similar conditions. The results obtained are presented in Table 2. After completion of the third cycle, a decrease of approximately 20% was observed in the photocatalytic activity of the catalyst.

3.5. Effect of initial pH of the dye solution

The solution pH appears to play an important role in the photocatalytic process of various pollutants [25,26]. The effect of pH on the photocatalytic degradation of BR2 was investigated in the pH range 5.0–11.6.The pH of the solution is adjusted before irradiation

Table 2
Effect of recycling on the photocatalytic activity of WO_3 synthesized by ppt method for the degradation of Safranin-O.

Number of cycle	k (min^{-1})	r^2	Degradation rates (mM min^{-1})
0	0.2614	0.9875	0.1489
1st cycle	0.2473	0.9922	0.1409
2nd cycle	0.2314	0.9939	0.1319
3rd cycle	0.2102	0.9875	0.1198

Table 3
Effect of dye concentration on photocatalytic degradation of BR2 using nanocrystalline WO_3 prepared by ppt method.

Initial dye conc. $\times 10^{-4}$ mol L^{-1}	k (min^{-1})	r^2	Photodegradation rate $\times 10^{-5}$
2.85	0.5737	0.9790	16.35
5.70	0.2483	0.9633	14.15
8.55	0.0609	0.9801	5.21
11.4	0.0479	0.9860	5.46
14.25	0.0335	0.9811	4.77

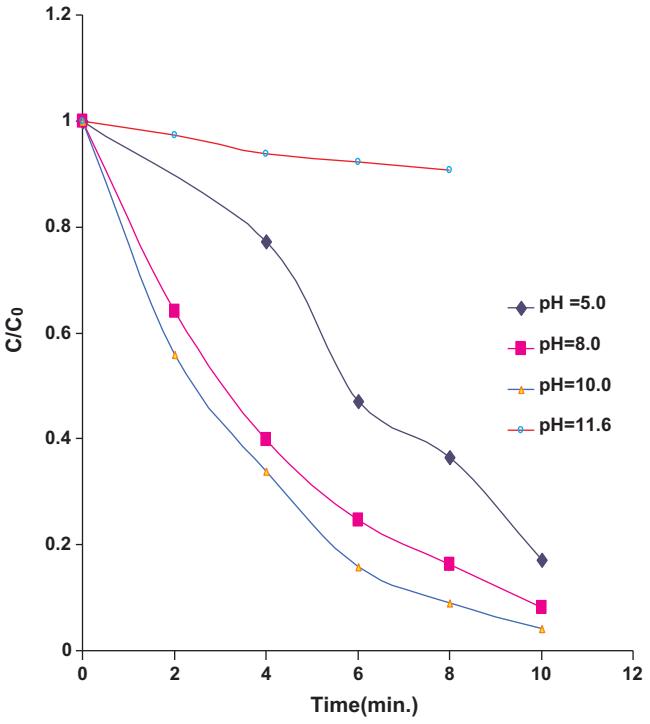

Fig. 13. A plot showing change of photodegradation rate with the increase in pH.

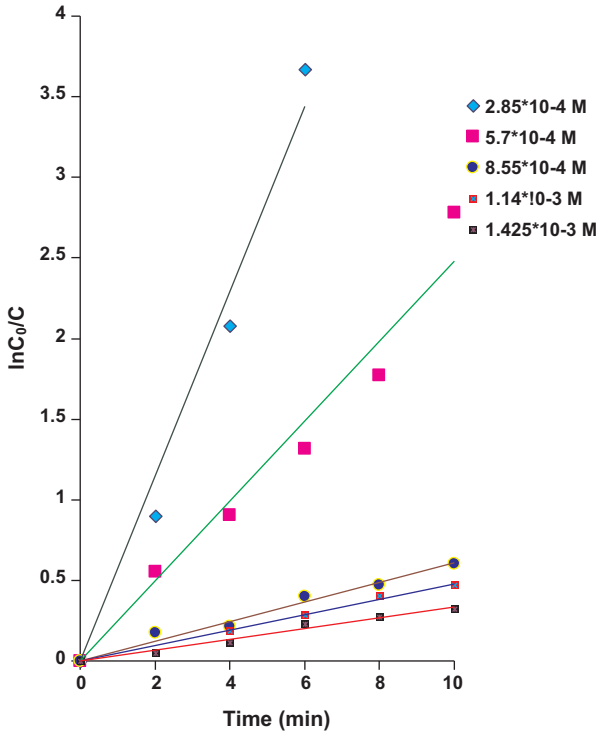

Fig. 14. A plot of ln C_0/C versus laser irradiation time for an aqueous solution of BR2 representing the effect of the initial dye concentration.

and it is not controlled during the course of the reaction. Fig. 13 depicts that the degradation efficiency increases with increase in pH from 5 to 10 and then decreases with further increase in pH. At acidic pH range the removal efficiency is less and it is due to the dissolution of WO_3. So the optimum pH for efficient BR2 removal is pH 10.0. The pH influences not only the surface properties of the photocatalyst but also the dye dissociation and OH radical formation. The values of degradation rates obtained are listed in Table 1. The photocatalytic degradation rate was found to increase with the increase in reaction pH and maximum photocatalytic degradation was achieved at 10.0 pH as shown in Fig. 13.

The possible reason for the different reaction rates at different pH values may be correlated to the generation of active hydroxyl radicals and occupancy of active sites of catalyst surface for the production of $OH^{\bullet}$ radicals by intermediate products. Values of solution pH can alter the degradation route and lead the formation of different intermediate products [27]. Based on the photocatalytic mechanism, the active $OH^{\bullet}$ radicals are produced on the surface of catalyst by the reaction of h^+ and adsorbed OH^-. During the course of photocatalytic reactions, formation of some negatively charged species (e.g., intermediate products) can occur and compete with OH^- for occupancy of catalyst surface. This competition reduces the possibility of adsorption of OH^- on the surface of catalyst which, in turn, affect the generation of active $OH^{\bullet}$ thereby decreasing the efficiency of the process. The isoelectric point (pHIEP) corresponds to the zeta potential equal to zero. The surface of photocatalyst was charged positively under pH < pHIEP. The dye used in this study was cationic dye and was positively charged under experimental conditions. Accordingly, electrostatic interactions between the photocatalyst surface and dye cation lead to the formation of little adsorption at low pH range. Gomes Silva and Luís Faria [28] observed the same trend for the photocatalytic degradation of phenol using nanocrystalline TiO_2.This phenomenon may occur because of the cationic nature of the dye. OH radical formation might be suppressed at more alkaline pH and the degradation rate of the dye is decreased. Because several reaction mechanisms can contribute to dye degradation, including OH radical attack, direct oxidation by the positive holes, and direct reduction by the electrons, the effect of pH on degradation efficiency differs from that of photocatalysts and photodegradation model substrates.

3.6. *Effect of substrate concentration*

In order to investigate the influence of initial dyes concentration on the degradation rate, the various initial dye concentrations were used. The initial concentration of the Safranin-O (SO) was varied from 2.85×10^{-4} M to 1.425×10^{-3} M. In all cases, 100 mL of the dye solutions containing 1.0 g L^{-1} of naocrystalline WO_3 were irradiated. The observed data were plotted as the experimental rate constant versus initial dye concentration. The results obtained are shown in Fig. 14 and presented in Table 3. It was observed that for this range of concentrations the reaction rate gets slower as the initial concentration of the dye in solution increases. As the concentration of SO increases, more reactant and reaction intermediates are adsorbed on the surface of the photocatalyst, therefore, the generation of hydroxyl radicals will be reduced because only a fewer active sites are available for adsorption of hydroxyl anions. The removal rate decreases with the increase in concentration of the dye. Similar results have been reported for the photocatalytic oxidation of other dyes [29]. Increase in the concentration of dye from 2.85×10^{-4} M to 1.425×10^{-3} M decreases the rate constant from 0.5737 to 0.0355 min^{-1} in 10 min.

The linearity of the function with high values of r^2 was observed for all investigated dyes but only in the limited range of their C_0 .The rate constant varies considerably with the increase in the initial dye concentration. It was found that when the initial concentration of the dye was high, their k were significantly lower as compared to the lower concentration of the dye. The possible explanation for this behavior is that as the initial concentration of the dye increases, the path length of the photons entering the solution decreases and in low concentration the reverse effect is observed, thereby increasing the number of photon absorption by the catalyst in lower concentration [30–32]. At high concentration of dye, the dye molecules

may absorb a significant amount of light rather than the catalyst and this may also reduce the catalytic efficiency [33]. The same effect was observed by Neppolian et al. [34] during the photocatalytic degradation of three commercial textile dyes using TiO_2 as photocatalyst under solar light.

4. Conclusions

Safranin-O is carcinogenic and the rate of the removal of the dye using nanocrystalline WO_3 is very high as compared to the conventional UV lamps. Laser induced photocatalysis is more efficient and could be used for the degradation of toxic organic pollutants. Experimental results demonstrate that the maximum degradation of the dye was achieved at pH 10.0. The optimum dye concentration, the amount of catalyst and laser energy used in our experiment were 0.57 mM, 1.0 g L^{-1} and 140 mJ. A linear increase in dye degradation was observed with the increase in laser energy up to certain level. The removal of the dye was achieved with a degradation rate = 1.46×10^{-4} M min^{-1} which is quite high as compared with rates reported for conventional UV lamps. This study clearly demonstrates that the laser-induced photocatalytic process could be able to degrade organic pollutants present in waste water in shorter time durations as compared to conventional setups. The optimization of various operational parameters is beneficial to increase the degradation efficiency.

References

[1] O. Ligrini, E. Oliveos, A. Braun, Photochemical processes for water treatment, Chem. Rev. 93 (1993) 671–698.
[2] M. Boeningo, Carcinogenicity and Metabolism of Azodyes Especially Those Derived From Benzidine, DNHS (NIOSH) publication, U.S Gov. Printing Off., Washington, DC, 1994, pp. 80–119.
[3] C.T. Helmes, C.C. Sigman, Z.A. Fund, M.K. Thomson, M.K. Voeltz, M. Makie, A study of azo and nitro dyes for the selection of candidates for carcinogen bioassay, J. Environ. Sci. Health A 19 (1984) 97–231.
[4] I. Arslam, I.A. Balcioglou, T. Tuhkanen, D. Bahnemann, Photochemical and photocatalytic detoxification of reactive dye bath wastewater by the Fenton's reagent and novel TiO_2 powders, J. Environ. Eng. 126 (2000) 903–911.
[5] N. Stock, J. Peller, K. Vinodgopal, P.V. Kamat, Combinative sonolysis and photocatalysis for textile dye degradation, Environ. Sci. Technol. 34 (2000) 1747–1750.
[6] E. Puzenak, H. Lachheb, M. Karkinaz, C. Guillard, J.M. Hermann, Fate of Nitrogen atoms in the photocatalytic degradation of Congo red, J. Photoenergy 5 (2003) 51–55.
[7] M.A. Fox, M.T. Dulay, Heterogeneous photocatalysis, Chem. Rev. 93 (1993) 341–357.
[8] E. Kusvuran, A. Samil, O.M. Atanur, O. Erbatur, Photocatalytic degradation kinetics of di- and tri-substituted phenolic compounds in aqueous solution by TiO_2/UV, Appl. Catal. B: Environ. 58 (2005) 211–216.
[9] S. Lathasree, R. Nageswara, B. Sivasankar, V. Sadasivan, K. Rengaraji, Heterogeneous photocatalytic mineralization of phenols in aqueous solutions, J. Mol. Catal. A: Chem. 223 (2004) 101–105.
[10] C.G. Silva, J.L. Faria, Photochemical and photocatalytic degradation of an azo dye in aqueous solution by UV irradiation, J. Photochem. Photobiol. A: Chem. 155 (2003) 133–143.
[11] L.W. Miller, M.I. Tejedor, M.A. Anderson, Titanium dioxide-coated silica waveguides for the photocatalytic oxidation of formic acid in water, Environ. Sci. Technol. 33 (1999) 2070–2075.
[12] I. Poulios, I. Tsachpinis, Photodegradation of the textile dye Reactive Black 5 in the presence of semiconducting oxides, J. Chem. Technol. Biotechnol. 74 (1999) 349–357.
[13] A. Pandurangan, P. Kamala, S. Uma, M. Palanichamy, V. Murugesan, Degradation of Basic Yellow auramino-A textile dye by semiconductor photocatalysis, Indian J. Chem. Technol. 8 (2001) 496–499.
[14] L.B. Reutergardh, M. Iangphasuk, Photocatalytic decolorization of reactive azo dyes: a comparison between TiO_2 and CdS, Chemosphere 35 (3) (1997) 585–596.
[15] S. Supothina, P. Seeharaj, S. Yoriya, M. Sriyudthsak, Ceram. Int. 33 (2007) 931–936.
[16] K. Demeestere, J. Dewulf, H. Van Langenhove, B. Sercu, Chem. Eng. Sci. 58 (2003) 2255–2267.
[17] A. Hameed, M.A. Gondal, Z.H. Yamani, Effect of transition metal doping on photocatalytic activity of WO_3 under laser illumination: role of 3d-orbitals, Catal. Commun. 5 (2004) 715–719.
[18] M.A. Gondal, A. Hameed, A. Al-Suwaiyan, Photocatalytic conversion of methane into methanol using visible laser, Appl. Catal. A 243 (2003) 165–174.
[19] C.H. Wu, H.W. Chang, J.M. Chern, Basic dye decomposition kinetics in a photocatalytic slurry reactor, J. Hazard. Mater. B 137 (2006) 336–343.
[20] W.Z. Tang, H. An, Photocatalytic degradation kinetics and mechanism of acid blue 40 by TiO_2/UV in aqueous solution, Chemosphere 31 (1995) 4171–4183.
[21] M.R. Hoffmann, S.T. Martin, W. Choi, D.W. Bahnemann, Environmental applications of semiconductor photocatalysis, Chem. Rev. 95 (1995) 69–96.
[22] H. Matsutani, S. Takasaki, Photocatalytic decomposition rate of TOC with suspended platinum loaded TiO_2 within internal radiation-type cylindrical reactors, Jpn. Soc. Water Environ. 19 (1996) 236–242.
[23] A. Akyol, H.C. Yatmaz, M. Bayramoglu, Photocatalytic decolorization of Remazol Red RR in aqueous ZnO suspensions, Appl. Catal. B: Environ. 54 (2004) 19–24.
[24] N. Daneshvar, D. Salari, A.R. Khataee, Photocatalytic degradation of azo dye acid red 14 in water on ZnO as an alternative catalyst to TiO_2, J. Photochem. Photobiol. A: Chem. 157 (2003) 111–116.
[25] S. Sakthivel, B. Neppolian, M.V. Shankar, B. Arabindoo, M. Palanichamy, V. Murugesan, Solar photocatalytic degradation of azo dye: comparison of photocatalytic efficiency of ZnO and TiO_2, Sol. Energy Mater. Sol. Cells 77 (2003) 65–82.
[26] C. Lizama, J. Freer, J. Baeza, H.D. Mansilla, Optimized photodegradation of Reactive Blue 19 on TiO_2 and ZnO suspensions, Catal. Today 76 (2002) 235–246.
[27] M.S.T. Gonclaves, A.M.F. Oliveira-Campose, E.M.M.S. Pinto, P.M.S. Plasencia, M.J.R.P. Queiroz, Photochemical treatment of solutions of azo dyes containing TiO_2, Chemosphere 39 (1999) 781–786.
[28] C. Gomes Silva, J. Luís Faria, Effect of key operational parameters on the photocatalytic oxidation of phenol by nanocrystalline sol–gel TiO_2 under UV irradiation, J. Mol. Catal. A: Chem. 305 (2009) 147–154.
[29] I. Poulios, I. Aetopoulou, Photocatalytic degradation of the textile dye Reactive Orange 16 in the presence of TiO_2 suspensions, Environ. Technol. 20 (1999) 479–487.
[30] E. Bizani, K. Fytianos, I. Poulios, V. Tsiridis, Photocatalytic decolorization and degradation of dye solutions and wastewaters in the presence of titanium dioxide, J. Hazard. Mater. 136 (2006) 85–94.
[31] J. Zhao, T. Wu, K. Wu, K. Oikawa, H. Hidaka, N. Serpone, Photo assisted degradation of dye pollutants 3: evidence for the need for substrate adsorption on TiO_2 particles, Environ. Sci. Technol. 32 (1998) 2394–2400.
[32] R.J. Davis, J.L. Gainer, G.O. Neal, I.W. Wu, Photocatalytic decolorization of wastewater dyes, Water Environ. Res. 66 (1994) 50–53.
[33] A. Mills, R.H. Davis, D. Worsely, Water purification by semiconductor photocatalysis, Chem. Soc. Rev. 22 (1993) 417–425.
[34] B. Neppolian, H.C. Choi, S. Sakthivel, B. Arabindoo, V. Murugesan, Solar/UV-induced photocatalytic degradation of three commercial textile dyes, J. Hazard. Mater. B 89 (2002) 303–317.